# Noncoherent Ultra Wideband Wireless Sensor Networks for Primary User Detection

Yağmur Sabucu
Faculty of Electrical and Electronics Engineering
Boğaziçi University
Istanbul, Turkey,
Email: sabucu@itu.edu.tr

Serhat Erküçük
Faculty of Engineering and Natural Sciences
Kadir Has University
Istanbul, Turkey
Email: serkucuk@khas.edu.tr

***Abstract*—As a result of increasing demand for new technologies, unlicensed usage of available spectrum has become very essential to provide an efficient usage of spectrum. For that reason, sensor networks may be a reliable option to decide on the absence/presence of licensed users and to communicate without causing much interference as a secondary user network. These networks consist of two communication links for primary user detection. One link is between the primary user and the sensors, and the other link is between the sensors and the fusion center. In this study, we consider an IEEE 802.15.4a based ultra wideband (UWB) network with a noncoherent receiver structure for the first link. For the second link binary pulse position modulation is implemented to convey primary user information to the fusion center. Numerical expressions for probabilities of false alarm and detection for the overall system are obtained and validated by simulations, where the performance of the system improves with number of sensors and the reliability of the first link. The results obtained from this study can be used for improving the primary user detection performance of UWB based wireless sensor networks in noncoherent operation mode.**

## I. Introduction

With the growing demand on wireless communication systems, challenges of the usage of limited resources increase at a tremendous rate. Energy efficiency, spectrum efficiency, interference management and reliability are some of the most important challenges in wireless communication systems [1]. Wireless Sensor Networks (WSNs) are mostly preferred for their energy efficiency even under low signal-to-noise ratios. Although unreliable communication channels may cause significantly high bit error rates, this problem can be solved using some robust approaches or technologies [2]. In WSNs, fusion center structures and the decision mechanisms are the most important factors that affect the overall system performance [3]. In [4], decision mechanisms are presented in orthogonal multiple access channels. In addition to decision mechanisms, optimum fusion rules have been investigated under some assumptions such as conditional independence [5], [6].

Another important issue for the WSNs is the coexistence of a secondary network with a primary user or a network. As an underlaying secondary system, ultra wideband (UWB) systems have been proposed [7], which are preferred in many applications due to their low complexity, low cost and high robustness to interference. UWB systems achieve robustness to interference by spreading their transmit spectrum above 500 MHz. On the other hand, despite being underlay systems many regulatory agencies require UWB systems to detect the presence of a primary user in order not to cause interference. The reliability in assessing the primary user's activity (i.e., being active or passive) may be enhanced using multiple UWB systems in a WSN. In [8], noncoherent receivers and multiple access channel related scenarios are investigated for power consumption under Rician and Rayleigh fading channels in WSNs. In [9], distributed detection in UWB based WSNs is studied including the energy budget and the effect of bandwidth under frequency selective channels. In [10], the effects of binary pulse position modulation (BPPM) and BPPM/binary phase shift keying (BPPM/BPSK) on a UWB based WSNs are investigated for primary user detection through simulation studies, where each user transmits through orthogonal channels.

In this paper, unlike earlier UWB based primary user (PU) detection studies, standardized IEEE 802.15.4a based UWB systems [11] are considered to detect the absence/presence of the PUs with a noncoherent receiver and a BPPM transmitter structure, to provide realistic detection results. The PU activity information is assessed by the noncoherent structure of each sensor, where the local decisions are transmitted to the fusion center. In the proposed model, the fusion center does not require any complex fusion rule as each sensor transmits simultaneously its decision using BPPM either in the first or the second half of the symbol duration. Therefore, such a noncoherent receiver structure at the fusion center deciding the PU activity directly on the received signal energy decreases the energy consumption and computational complexity significantly. Numerical expressions are obtained for the probabilities of false alarm and misdetection for the overall system, and the detection performance is investigated for various link reliability cases and different number of sensors. The probabilities of false alarm and misdetection expressions are accurate and confirmed by simulations for various scenarios.

The paper is organized as follows. In Section II, system model is explained in detail for the primary user-sensor link, sensor-fusion center link and the decision rule. In Section III, the proposed system is analyzed and expressions are obtained for probabilities of false alarm and detection for the overall

978-1-4673-8818-4/16/$31.00 ©2016 IEEE

ISSN: 2157-023X

system. In Section IV, both simulation and analytical results are presented for different number of sensors and various reliability of the links, confirming the validity of the analysis. In Section V, concluding remarks are given.

## II. System Model

The proposed primary user detection structure consists of two cascade links; between licensed user-sensors and sensors-fusion center, as seen in Fig. 1. Sensors observe the primary user's activity, make local decisions and then transmit their binary decisions (representing absence and presence) to the fusion center using BPPM signalling. As in [12], sensors listen to either uplink or downlink of the primary system simultaneously to decide on the activity of primary user in that specific band. In the first link, the absence/presence information is decided at each sensor and the detection performance is explained with respect to the two hypotheses, which are given in Section II-A. In the second link, the local active or passive decisions are transmitted individually by UWB systems using BPPM signalling to the fusion center that has a noncoherent receiver structure and a decision is reached at the fusion center, which are explained in Section II-B.

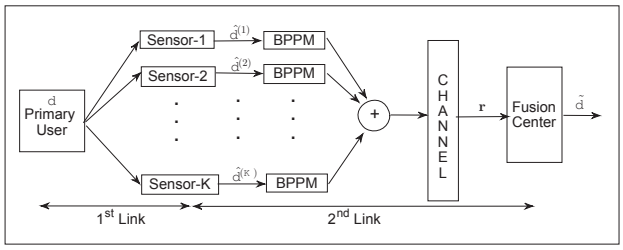


Fig. 1. A UWB based WSN system with noncoherent receiver structure

### A. Primary User - Sensor Link Structure

In the first link, each sensor decides individually on the absence/presence of the primary user. The absence or the presence of the primary user is represented by two hypotheses, $H_0$ and $H_1$, respectively as

$$H_0: \quad r_f(t) = n(t) \tag{1}$$

$$H_1: \quad r_f(t) = A\, e^{j\theta}\, w(t-\tau) + n(t). \tag{2}$$

Here, $r_f(t)$ represents the received signal in the first link, $\tau$ is the timing offset between the two systems, $w(t)$ is the primary user signal with amplitude $A$ and phase $\theta$ uniformly distributed over $[0, 2\pi)$, $n(t)$ is the additive white Gaussian noise (AWGN) with variance $\sigma_n^2 = N_0 W$, where $W$ and $N_0$ are the transmission bandwidth and noise power spectral density, respectively.

The decision variable for the system is obtained as $d = \frac{2}{N_0}\int_0^T |r_f(t)|^2\, dt$, where $T$ is the integration time for the system and $|\cdot|$ is the absolute value operator. The UWB receiver at each sensor compares the decision variable $d$ to a pre-selected threshold value $\lambda$ in order to take an action. Assuming the sensors are identical and the signal-to-noise ratios (SNRs) are similar, the same threshold value is used at each sensor. Accordingly, by adjusting the threshold value, $\lambda$, the performance measures, probability of false alarm and probability of detection, for each identical system can be expressed as

$$P_f = \Pr[d > \lambda | H_0] \tag{3}$$

$$P_d = \Pr[d > \lambda | H_1], \tag{4}$$

respectively. When the primary system is active, the decision variable $d$ has a central $\chi^2$-distribution[1] with $N = 2TW$ degrees of freedom (DOF) and variance $\sigma^2 = \gamma + 1$, where $\gamma = \frac{A^2\sigma_s^2}{N_0 W}$ is the SNR, $\sigma_s^2$ is the variance of the primary signal samples, and the additional term "1" corresponds to the normalized noise samples. When the primary system is inactive, the variance becomes $\sigma^2 = 1$. Thus, the probability density function (pdf) of $d$ for either hypothesis can be expressed as

$$f_{_D}(d) = \frac{1}{\sigma^N\, 2^{N/2}\, \Gamma(N/2)}\, d^{N/2-1} e^{-d/2\sigma^2}, \tag{5}$$

where $\Gamma(a,b) = \int_b^\infty e^{-t} t^{a-1} dt$ is the upper incomplete Gamma function and $\Gamma(a) = \Gamma(a,0)$ is the Gamma function [13]. Based on (5) both probabilities, $P_f$ and $P_d$, for each sensor can be obtained as

$$P_x = Q\left(\frac{N}{2}, \frac{\lambda}{2\sigma^2}\right) = \frac{\Gamma\left(\frac{N}{2}, \frac{\lambda}{2\sigma^2}\right)}{\Gamma\left(\frac{N}{2}\right)} \tag{6}$$

with the corresponding $\sigma^2$ values for $H_0$ and $H_1$, where $x \in \{f, d\}$ and $Q(a,b)$ is the regularized upper incomplete Gamma function [13]. At each sensor, independent decisions $\hat{d}^{(k)} \in \{0, 1\}$ for $k = \{1, 2, \ldots K\}$ can be reached where $\hat{d}^{(k)} = 0$ implies the decision "absent" and $\hat{d}^{(k)} = 1$ implies the decision "present" for a primary user.

### B. Sensor-Fusion Center Link Structure

From each sensor, one-bit local decisions $\{\hat{d}^{(k)}\}$ are transmitted with BPPM to the fusion center through the second link. BPPM uses a signal with a constant amplitude and constant width, and positions the primary user signal information on a related position based on the local decision. Assuming all sensors transmit synchronously, the BPPM received signal can be expressed as

$$r(t) = \sum_{k=1}^{K} s^{(k)}(t) * h^{(k)}(t) + n(t), \tag{7}$$

where $s^{(k)}(t)$ is the transmitted symbol of the $k^{th}$ sensor containing the estimated binary $\hat{d}^{(k)}$ information (absent/present) and is represented as

$$s^{(k)}(t) = p\left(t - \hat{d}^{(k)}\frac{T_s}{2}\right) \tag{8}$$

[1]Primary user signal samples are assumed to be Gaussian distributed.

with $T_s$ being the duration of the received signal. $h^{(k)}(t)$ represents $k^{th}$ sensor's channel as given in [14]

$$h^{(k)}(t) = \sum_{n=1}^{N} h_n^{(k)} \delta(t - nT_p), \tag{9}$$

where $T_p$ is the channel resolution and the pulse duration, and $N$ is the number of multipath coefficients. To prevent inter-symbol interference, it is assumed that $NT_p \leq T_s/2$. The channel coefficients of the $k^{th}$ user are $\mathbf{h}^{(k)} = [h_1^{(k)} h_2^{(k)} ... h_N^{(k)}]^T$, where $N$ is the length of discrete-time equivalent channel. In practice, the double exponential decay model is used for the modeling of UWB channels, however, obtaining performance expressions in such channels are not trivial mathematically. For mathematical tractability, the Gaussian approximation model is used in this study as in [14]. Accordingly, each channel coefficient is assumed to be Gaussian distributed with $h_n^{(k)} \sim N(0, \sigma_h^2)$ and the users' channels are independent and identically distributed.

To make a final decision, the instantaneous received energies of both positions are calculated and the accumulated energies are compared with each other. The position which has the maximum energy value is determined as the decision of the primary user's activity. In most conventional systems, it is assumed that each sensor's decision is assessed individually and the local decisions are processed with the majority rule to reach a final decision on the PU activity. In this study, assuming synchronous transmission of sensors, one-symbol duration is adequate to decide on the PU activity. The instantaneous received energy, $y_m$, which is the normalized signal energy by the noise power spectral density can be obtained for both positions $m = \{0, 1\}$ as

$$y_m = \frac{2}{N_0} \int_{m\frac{T_s}{2}}^{(m+1)\frac{T_s}{2}} |r(t)|^2 dt. \tag{10}$$

Comparing energy values $y_0$ and $y_1$, a decision on PU activity will be reached at the fusion center. Accordingly, if $y_1$ is larger than $y_0$, a decision that PU is active, will be given. Therefore, the probabilities of false alarm and detection of the overall system can be expressed as

$$\begin{aligned} P_F &= \Pr[\acute{y} < 0 \mid H_0] \\ P_D &= \Pr[\acute{y} < 0 \mid H_1] \end{aligned} \tag{11}$$

where $\acute{y} = y_0 - y_1$. The probabilities of detection and false alarm of the overall system will depend on the qualities of both links and number of sensors. This will be discussed in the Results section. Next, system analysis of the proposed PU detection approach is presented.

## III. System Analysis

For analysis purposes, the discrete-time equivalent model to compute instantaneous received energy, $y_m$, can be written as

$$y_m = \frac{2}{N_0} \mathbf{r}_m^T \mathbf{r}_m, \tag{12}$$

where the $2N \times 1$ received vector $\mathbf{r}$ is the concatenation of $N \times 1$ vectors $\mathbf{r}_0$ and $\mathbf{r}_1$, $\mathbf{r} = [\mathbf{r}_0 \mathbf{r}_1]$, given as

$$\mathbf{r}_m = \mathbf{S}\mathbf{h} + \mathbf{n}, \quad m = \{0, 1\}, \tag{13}$$

where $\mathbf{S}^{R \in (N \times N)}$ is an $N \times N$ scalar matrix representing time-shifted pulses and $\mathbf{h}$ represents the combined effective channel and pulse position information for all $K$ users. Since the elements of both $\mathbf{h}$ and $\mathbf{n}$ are Gaussian distributed, each element of $\mathbf{r}_m$ is zero mean and has a variance of $\sigma_{r_0}^2 = \sigma_h^2(K - i) + \sigma_n^2 K$ for $m = 0$ (i.e., position "0") and $\sigma_{r_1}^2 = \sigma_h^2 i + \sigma_n^2 K$ for $m = 1$ (i.e., position "1"), respectively. Here, $i$ and $(K - i)$ represent the number of sensors transmitting the binary information "1" and "0", respectively. Therefore, the variable $y_m$ for positions $m = 0$ and $m = 1$ depending on $i$ can be modelled with central $\chi^2$-distribution with $N$ degrees of freedom as in [15] and [16] by using (5) as

$$f_{Y_{0,i}}(y) = \frac{y^{N/2-1} e^{-y/2\{\sigma_h^2(K-i) + \sigma_n^2 K\}}}{\{\sigma_h^2(K-i) + \sigma_n^2 K\}^{N/2} 2^{N/2} \Gamma(N/2)} \tag{14}$$

$$f_{Y_{1,i}}(y) = \frac{y^{N/2-1} e^{-y/2\{\sigma_h^2 i + \sigma_n^2 K\}}}{\{\sigma_h^2 i + \sigma_n^2 K\}^{N/2} 2^{N/2} \Gamma(N/2)}. \tag{15}$$

In classical approach, a predefined threshold value is chosen and a final decision is given by comparing the collected energy with this threshold [15], [16]. Therefore, obtaining an effective threshold is an important factor which affects directly the performance of the system. Different from these studies, the comparison of the collected energies for the two positions can be simply used to make a PU activity decision in this study. The probability of active decision (i.e., PU is active) can be calculated by using the distributions related to each position depending on $i$. Accordingly, pdf of $\acute{y} = y_0 - y_1$ can be calculated as the convolution of two pdfs. Hence, the probability of active decision can be calculated depending on $i$ as

$$P_{act,i} = \int_{-\infty}^{0} \int_{-\infty}^{\infty} f_{y_{0,i}}(v) f_{y_{1,i}}((\acute{y} + v)) dv d\acute{y}. \tag{16}$$

In Fig. 2, the pdf of $\acute{y}$ and the calculation of the probability of active decision are illustrated for $K = 3$ and $i = 0$ when $SNR = 0$ dB. Note that (16) and the simulation of the second link depending on $i$ are in well correspondence.

For the overall detection performance of the system, the number of active decisions, $i$, in the first link is also important. The probabilities of active decisions of the first link conditioned on hypotheses are obtained as [16]

$$\begin{aligned} P(i|H_0) &= \binom{K}{i} P_f^i (1 - P_f)^{(K-i)} \\ P(i|H_1) &= \binom{K}{i} P_d^i (1 - P_d)^{(K-i)} \end{aligned} \tag{17}$$

where $i$ is the number of active decisions of $K$ sensors. Accordingly, the probability of deciding "active" for the overall

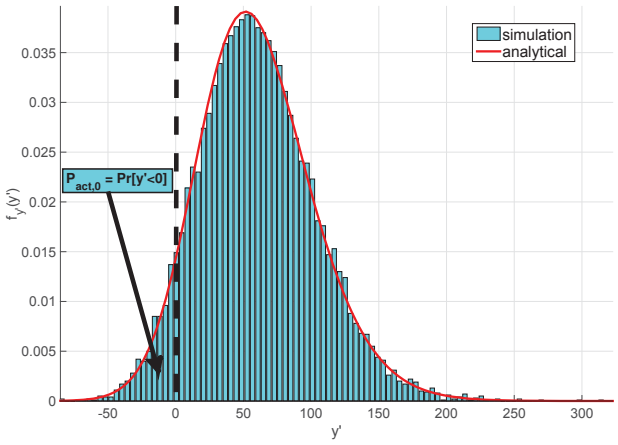


Fig. 2. Pdf of $\acute{y}$ for $K = 3$ and $i = 0$ when $SNR = 0$ dB.

system can be obtained by using (16) and (17) considering all $i$ cases as

$$\begin{aligned} P_F &= \textstyle\sum_{i=0}^{K} P_{act,i} P(i|H_0) \\ P_D &= \textstyle\sum_{i=0}^{K} P_{act,i} P(i|H_1) \end{aligned} \tag{18}$$

In addition to $P_F$ and $P_D$, a converged value is obtained for the overall system performance when the second link is assumed as noise-free[2] and can be written as

$$P_{X_{conv}} = \sum_{i=\lceil K+1/2 \rceil}^{K} \binom{K}{i} P_x^i (1-P_x)^{(K-i)} + F_{eo} \tag{19}$$

where $X \in \{F, D\}$, $x \in \{f, d\}$, $\lceil . \rceil$ is the ceiling operator, and $F_{eo}$ represents a factor that depends on even/odd situation of $K$ defined as

$$F_{eo} = \begin{cases} \frac{1}{2}\binom{K}{K/2} P_x^{K/2}(1-P_x)^{(K/2)}, & \text{if } K : even \\ 0 \qquad\qquad\qquad\qquad\quad , & \text{if } K : odd. \end{cases} \tag{20}$$

## IV. Results

In this section, the theoretical results are verified by simulations for different scenarios. The detection performance of a UWB sensor network with BPPM signalling is investigated under various first link situations, number of sensors, and reliability of the second link when the channel length is assumed as $N = 20$. The overall probability of false alarm, $P_F$, and probability of misdetection, $P_{MD} = 1 - P_D$, are obtained by considering (11) and (18). The primary user is assumed to have only an uplink channel. $K$ sensors listen to the licensed user and decide on the activity of the PU by using Neyman-Pearson (NP) test as in [12]. These binary decisions are transmitted by BPPM to the fusion center through the second link. The fusion center reaches an overall decision.

In Fig. 3, probability of false alarm of the overall system, $P_F$, is illustrated for various number of sensors under different SNRs of the second link. The probability of false alarm of the first link, $P_f$, is 0.01. $P_F$ reaches an error floor when different number of sensors listen to the spectrum of the primary user as SNR increases. The error floors for different number of sensors can be calculated as in (19). The lowest $P_F$ for 1-sensor system converges to $P_f$ as SNR increases in the second link. In addition, the performance of the system improves compared to the first link as the number of sensors in the system increases. The error floors can be reached between $[0, 10]$ dB SNR depending on number of sensors as seen in Fig. 3. Also, it should be noted that theoretical and simulation results match well.

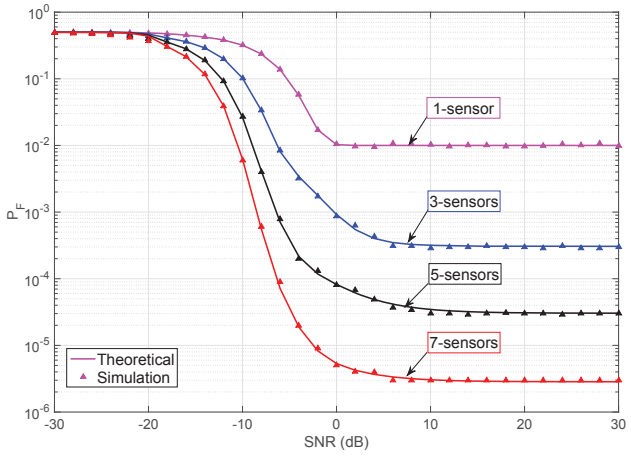


Fig. 3. Probability of false alarm ($P_F$) of the overall system when 1st Link's $P_f$ is 0.01 for 1,3,5, and 7 number of sensors

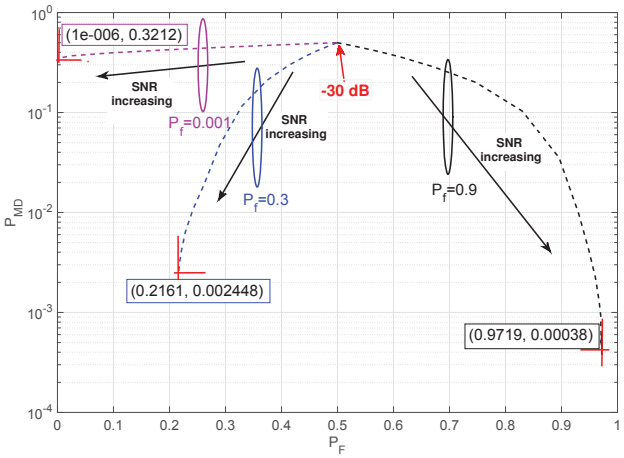


Fig. 4. Probability of misdetection ($P_{MD}$) and false alarm ($P_F$) of the overall system for various $P_f$ of the 1st Link

The trade-off between the probability of misdetection, $P_{MD}$, and false alarm, $P_F$, of the overall system is shown for different first channel reliability conditions in Fig. 4. Primary user's channel is assumed to have an SNR of 5 dB. The performance of the overall system is assessed for three different reliability conditions of the first link, $P_f = \{0.001, 0.3, 0.9\}$, resulting in $P_{md} = \{0.3784, 0.0287, 0.0009\}$. It is assumed that $K = 3$ sensors listen to the PU spectrum. Simulations are

[2]Although the second link is assumed to be noise-free, multipath channel still affects the signal components.

performed on a wide range of SNR values $[-30, 30]$ dB for the second link. When $SNR = -30$ dB, the second link is very unreliable so all cases converge to $50\%$ probability of false alarm and misdetection as expected. When $SNR = 30$ dB, the second link is almost noiseless so $P_F$ and $P_{MD}$ converge to probability values which are also confirmed by (19). An observation regarding $(P_F, P_{MD})$-pairs should be elaborated on. When the first link $P_f$ is high, while $P_F$ becomes worse, $P_{MD}$ much improves. While this will be to the advantage of the PU, the secondary users in the network will not be able to communicate efficiently. On the other hand, if $P_f$ is low, then the PU will be interfered more often in the overall system. Therefore, a better trade-off may be when $P_f$ is neither high nor low (e.g., $P_f = 0.3$).

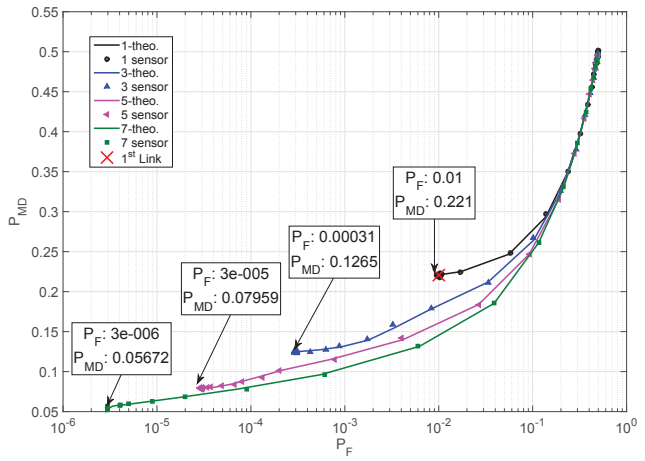


Fig. 5. Probability of misdetection ($P_{MD}$) and false alarm ($P_F$) of the overall system when the $P_f$ of 1st link is 0.01 for 1,3,5, and 7 sensors

Finally, Fig. 5 illustrates the overall performance improvement when the number of sensors is increased. All results in Fig. 5 are obtained in a wide SNR range of $[-30, 30]$ dB while assuming $P_f = 0.01$. The rate of improvement in reducing $P_F$ is much better compared to reducing $P_{MD}$ when the number of sensors is increased. For a high $P_f$ value in the first link, the rate of improvement would follow an opposite trend. In the figure, all numerical results are confirmed by simulations including the converged $(P_F, P_{MD})$ values. All in all, the improved detection performance can be calculated for various number of sensors in the proposed noncoherent UWB sensor network system.

## V. Conclusion

In this study, the PU detection performance of a noncoherent UWB system is studied considering PU-sensor and sensor-fusion center links. The UWB WSN system performs detection with different number of sensors and the local decisions are transmitted to the fusion center synchronously. It is shown that the analytical and simulation results match well and the information coming from the first link has a significant effect on the overall performance. Furthermore, as expected the performance of the overall system is improved by increasing the number of sensors. The results obtained in this study can be used for improving the primary user detection performance of the UWB based wireless sensor networks in noncoherent operation mode.

## Acknowledgment

This research was supported by 7th European Community Framework Programme-Marie Curie International Reintegration Grant and TUBITAK 2211-National Scholarship Programme for PhD Students.

## References

[1] A. Osseiran, V. Braun, T. Hidekazu, P. Marsch, H. Schotten, H. Tullberg, M. A. Uusitalo, and M. Schellman, "The foundation of the mobile and wireless communications system for 2020 and beyond: Challenges, enablers and technology solutions," in *IEEE Veh. Tech. Conf. (VTC)*, June 2013, pp. 1–5.

[2] B. Liu and B. Chen, "Channel-optimized quantizers for decentralized detection in sensor networks," *IEEE Trans. Info. Theory*, vol. 52, no. 7, pp. 3349–3358, July 2006.

[3] R. Jiang and B. Chen, "Fusion of censored decisions in wireless sensor networks," *IEEE Trans. Wireless Commun.*, vol. 4, no. 6, pp. 2668–2673, Nov. 2005.

[4] K. Liu and A. Sayeed, "Type-based decentralized detection in wireless sensor networks," *IEEE Trans. Signal Process.*, vol. 55, no. 5, pp. 1899–1910, May 2007.

[5] P. K. Varshney, *Distributed Detection and Data Fusion*, 1st ed. Secaucus, NJ, USA: Springer-Verlag New York, Inc., 1996.

[6] Z. Chair and P. Varshney, "Optimal data fusion in multiple sensor detection systems," *IEEE Trans. Aerospace and Electr. Syst.*, vol. AES-22, no. 1, pp. 98–101, Jan. 1986.

[7] M. Win and R. Scholtz, "Ultra-wide bandwidth time-hopping spread-spectrum impulse radio for wireless multiple-access communications," *IEEE Trans. Commun.*, vol. 48, no. 4, pp. 679–689, Apr. 2000.

[8] F. Li, J. Evans, and S. Dey, "Decision fusion over noncoherent fading multiaccess channels," *IEEE Trans. Signal Process.*, vol. 59, no. 9, pp. 4367–4380, Sept. 2011.

[9] I. Oppermann, L. Stoica, A. Rabbachin, Z. Shelby, and J. Haapola, "UWB wireless sensor networks: UWEN - a practical example," *IEEE Commun. Mag.*, vol. 42, no. 12, pp. S27–S32, Dec. 2004.

[10] Y. Sabucu and S. Erkucuk, "Primary user detection in IEEE 802.15.4a based wireless sensor networks," in *Signal Process. and Commun. App. Conf. (SIU),*, Apr. 2013, pp. 1–4.

[11] "IEEE standard for information technology - telecommunications and information exchange between systems - local and metropolitan area networks - specific requirement part 15.4: Wireless medium access control (MAC) and physical layer (PHY) specifications for low-rate wireless personal area networks (WPANS)," *IEEE Std 802.15.4a-2007 (Amendment to IEEE Std 802.15.4-2006)*, pp. 1–203, 2007.

[12] S. Erkucuk, L. Lampe, and R. Schober, "Analysis of interference sensing for DAA UWB-IR systems," in *IEEE Intl. Conf. Ultra-Wideband, (ICUWB)*, vol. 3, Sept. 2008, pp. 17–20.

[13] M. Abramowitz and I. Stegun, *Handbook of Mathematical Functions: With Formulas, Graphs, and Mathematical Tables*, ser. Applied mathematics series. Dover Publications, 1964.

[14] K. Bai and C. Tepedelenlioglu, "Distributed detection in UWB wireless sensor networks," *IEEE Trans. Signal Process.*, vol. 58, no. 2, pp. 804–813, Feb. 2010.

[15] S. Erkucuk, L. Lampe, and R. Schober, "Joint detection of primary systems using UWB impulse radios," *IEEE Trans. Wireless Comm.*, vol. 10, no. 2, pp. 419–424, Feb. 2011.

[16] S. Yiu and R. Schober, "Nonorthogonal transmission and noncoherent fusion of censored decisions," *IEEE Trans. Veh. Tech.*, vol. 58, no. 1, pp. 263–273, Jan. 2009.